

## Dynamic Analysis of a Transmission Line Section Subject to Combined Conductor Breakage and Wind Loads

F. Alminhana<sup>1</sup>, F. Albermani<sup>1</sup> and M. Mason<sup>1</sup>

<sup>1</sup>School of Civil Engineering  
The University of Queensland, Queensland 4072, Australia

### Abstract

A worldwide survey carried out by CIGRÉ on transmission line (TL) failures showed that cascades, i.e., progressive collapse of line supports, play a pivotal role in the majority of TL structure collapses. Cascade triggering events can considerably magnify localized TL member failures, especially under wind and ice actions, resulting in the collapse of a large number of TL supports in many cases.

Phase conductor breakage is credited as the most severe cascade triggering event. These breakages generate a shock wave that propagates through the conductor, inducing large unbalanced longitudinal loads on TL supports. This article investigates the response of a TL section to a conductor breakage event, by means of a mechanical model developed to tackle such a problem, which employs nonlinear time-history dynamic analysis. Four different scenarios are considered, two of them isolating the effects of the triggering event and wind loading and the other two combining them.

### Introduction

Electrical energy outages caused by failure of transmission line supports are of concern to utilities worldwide. Support collapse, even partial, leads to prolonged and expensive energy disruptions, particularly in regions where the power grid lacks redundancy.

CIGRÉ (1996) carried out a survey of TL failures, focusing on supports and foundation failures, collecting data from 42 electrical utilities worldwide for failures that occurred over a period of 15 years (1981 to 1996). In total, 299 events encompassing the damage of 1731 structures were reported by the respondents, who also indicated the occurrence of cascades in many cases. Moreover, the survey data showed that a few events account for the majority of failed structures, clearly indicating the occurrence of cascades. More recent cascading events were reported by CIGRÉ (2012), where two events drew particular attention because of their calamitous aftermaths. These took place in Canada (1998) and France (1999), where a series of cascades were registered during severe storm events.

TL cascades are commonly classified in one of three categories (longitudinal, transverse and vertical), according to the direction of the damages. However, longitudinal cascades are the most severe and frequent type. They can be triggered by the failure of any of the components responsible for keeping the tension of conductors, or more frequently by the conductor itself, inducing large imbalanced loads in the adjacent structures.

The determination of the response of a TL section in a conductor breakage scenario is relatively challenging, because an abrupt change in the boundary conditions is introduced in the severed span. This generates singularities on the global stiffness matrix, and makes this type of problem difficult to solve by conventional finite element method (FEM). As a result, the use of an explicit direct integration method is required.

A mechanical model to numerically simulate coupled transmission line systems - supports, conductors, shield wires and insulators - subjected to a cable breakage event is presented in this article. The core of the model is the equations of motion solved through a central finite difference (CFD) scheme. This incorporates member nonlinearities and boundary condition changes. Additionally, an accurate cable element was introduced to simulate cable substructures, based on precise catenary relationships.

The model developed was employed to investigate the response of a transmission line section subjected to four different load cases (LCs): (i) ultimate limit state wind loading, (ii) conductor breakage only, (iii) serviceability limit state wind loading and conductor breakage, and (iv) ultimate limit state wind loading and conductor breakage.

A simplified wind loading model, following the code IEC60826 - IEC (2003), was employed to determine the wind effects on all components of the line section. This simplified approach is considered adequate because the investigation primarily focuses on the assessment of the response amplification caused by conductor breakage, not on the accurate prediction of wind loading.

### Mechanical model

The mechanical model deals with the transmission line system as a set of substructures: conductor and shield wire spans, supports and insulators. Each substructure is composed of an assembly of basic members, namely cable and truss elements.

Cable elements based on exact catenary relationships were introduced to deal with conductors and shield wire spans. Their formulation was deduced by applying equilibrium conditions to a cable span and incorporating linear elastic material relationships in a Lagrangian frame of reference (figure 1), resulting in the system of transcendental equations indicated in (1).

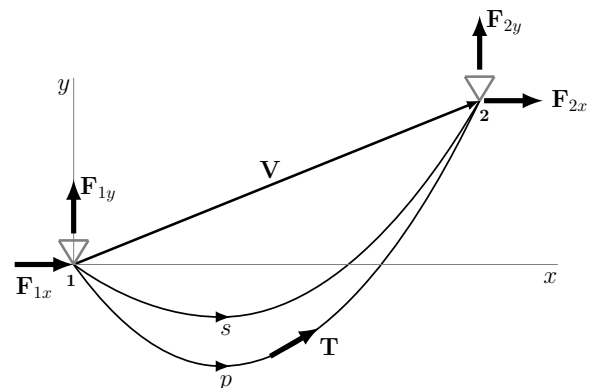


Figure 1: Catenary unstretched (*s*) and stretched (*p*) profiles.

$$-F_{1x} \left\{ \frac{L_o}{EA} + \frac{1}{w} [\ln(T_2 + F_{2y}) - \ln(T_1 - F_{1y})] \right\} = v_x^0 \quad (1a)$$

$$\frac{T_2^2 - T_1^2}{2EAw} + \frac{T_2 - T_1}{w} = v_y^0 \quad (1b)$$

where  $F_{1x}$ ,  $F_{1y}$ ,  $F_{2x}$ ,  $F_{2y}$  are the reactions at supports **1** and **2**, in the directions  $x$  and  $y$ , respectively;  $T_1$  and  $T_2$  are the axial cable forces at the supports;  $w$  is the uniformly distributed load applied over the cable length;  $L_o$  is the unstretched length of the cable;  $E$  is the elasticity modulus of the cable material;  $A$  is the cable cross-sectional area;  $v_x^0$  and  $v_y^0$  are the components of the chord vector  $\mathbf{V}$ .

All the force and tension terms contained in equations (1) can be expanded employing static equilibrium conditions, resulting in a system of transcendental equations depending only on the unknowns  $F_{1x}$  and  $F_{1y}$ . This system can not be solved explicitly, requiring an iterative strategy to achieve the solution. An incremental algorithm derived from Newton-Rapson's method is employed, as discussed below.

The process starts with an initial approximation for  $F_{1x}$  and  $F_{1y}$ , resulting in misclosure components ( $\Delta\mathbf{V}$ ) of the chord vector  $\mathbf{V}$ , obtained by differencing the left and right sides of each equation in (1). If the misclosure components are greater than a required tolerance ( $1 \times 10^{-6}$ ), corrections ( $\Delta\mathbf{F}_1$ ) for the values of  $F_{1x}$  and  $F_{1y}$  are calculated through the system represented by the vectorial equation:

$$\Delta\mathbf{V} = \mathbf{J}_V \Delta\mathbf{F}_1 \quad (2)$$

where  $\mathbf{J}_V$  is the Jacobian matrix of the system, composed by the partial derivatives of the left side of equation 1, in relation to the variables  $F_{1x}$  and  $F_{1y}$ . The system in (2) is algebraic (rank  $2 \times 2$ ) and can be easily solved. The correction terms  $\Delta\mathbf{F}_1$  are applied to  $F_{1x}$  and  $F_{1y}$ , and the misclosures are determined. The process is repeated until the tolerance limited is achieved.

In the procedure described, the member end forces vector  $\mathbf{F}$  are determined locally, in the plane of the catenary, which is spatially oriented according to the resultant vector of the wind and weight actions, and is coupled into the global three-dimensional system of reference by proper transformations.

Support structures and insulators are subassemblies of truss elements: two-node straight bars with three degrees-of-freedom (DOF) per joint, as indicated in figure 2. Each element is capable of resisting tension and compression axial forces, following a linear elastic constitutive relationship according to Hooke's law.

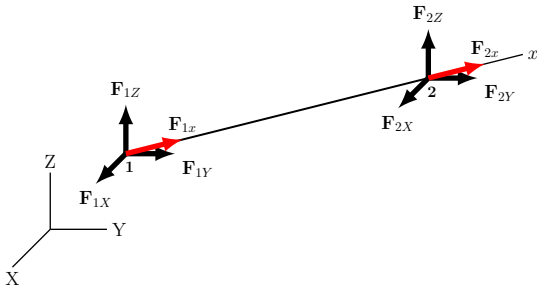


Figure 2: Three-dimensional truss element.

The dynamic response of the structural systems is determined by solving the equations of motion. In the case of linear elastic multi-degree-of-freedom (MDF) systems, assuming viscous damping, these equations are well-known and can be written in a

convenient matrix form:

$$\mathbf{M}\ddot{\mathbf{u}} + \mathbf{C}\dot{\mathbf{u}} + \mathbf{K}\mathbf{u} = \mathbf{P} \quad (3)$$

where:  $\mathbf{M}$ ,  $\mathbf{C}$  and  $\mathbf{K}$  are the matrices of mass, viscous damping and stiffness of the structure, respectively;  $\ddot{\mathbf{u}}$ ,  $\dot{\mathbf{u}}$  and  $\mathbf{u}$  are the time-depending vectors of acceleration, velocity and displacements; and  $\mathbf{P}$  is the vector of applied forces, also time dependent.

Because of nonlinearities, the global stiffness matrix ( $\mathbf{K}$ ) is dependent on the time history of displacement. Additionally, an abrupt change occurs in the boundary conditions as a result of element breakage, introducing singularities in  $\mathbf{K}$ , since part of the system becomes a mechanism. These changes in the stiffness matrix make the application of modal analysis not suited so a time-stepping scheme (direct integration) is more appropriate. This is done by employing a central finite difference (CFD) scheme. Succinctly, the CFD approach solves the equations of motion at discrete time intervals  $\Delta t$  apart, by replacing the velocity  $\dot{\mathbf{u}}$  and acceleration  $\ddot{\mathbf{u}}$  vectors in equation (3) by approximations based on finite differences of displacements in three time steps (two knowns and one unknown).

A lumped-mass approach, i.e., the distributed mass of the members is applied at the nodes, is adopted, resulting in a diagonalized matrix  $\mathbf{M}$ . A damping proportional to mass is assumed so the matrix  $\mathbf{C}$  also become diagonal. These two artifices uncouple equation (3), since the stiffness matrix multiplies the known vector of displacements  $\mathbf{u}_i$ .

Consequently, the system can be solved independently for each DOF, depending only on the latest known responses of the structure. In fact, it is not even necessary to assemble (or update) the global stiffness matrix of the structure so the matrix equation (3) can be reduced to a more convenient single-degree-of-freedom (SDF) form, resulting in the following recurring formula:

$$u_{i+1} = \frac{1}{1 + \frac{c_m \Delta t}{2}} \left[ \frac{r_i \Delta t^2}{m} + 2u_i - \left( 1 - \frac{c_m \Delta t}{2} \right) u_{i-1} \right] \quad (4)$$

where  $u_{i+1}$ ,  $u_i$  and  $u_{i-1}$  are the displacements at time steps  $(i+1)$ ,  $i$  and  $(i-1)$ , of a given DOF;  $m$  is the nodal mass;  $c_m$  is the proportionality constant between damping coefficient and nodal mass;  $r_i$  is resultant force acting on the DOF, obtained by the difference between the applied external load ( $p_i$ ) and the sum of the forces ( $\sum_{j=1}^N f_j^i$ ) of the  $N$  members connected to the node. The constant  $c_m = C/m$  combines the effects of the different sources of damping and is determined by assuming a damping ratio ( $\zeta$ ) according to the type of member. Because the structural response is determined using the system configuration of the previous time step as reference, the geometric nonlinearities are automatically accounted at each time step.

The central finite difference method is conditionally stable, producing meaningless results if the time step adopted is not short enough. According to Chopra (1995), the convergence and precision of the solution can be assured only if the time step  $\Delta t$  is less than a critical time step  $\Delta t_{crit} = T_n/\pi$ , where  $T_n$  is the smallest natural period of vibration of the system. This period must be determined, requiring modal dynamic analysis to calculate the eigenvalues of the system.

In order to overcome this difficulty, the approximated expression for  $\Delta t_{crit}$  given by Groehs (2001) is employed,

$$\Delta t \leq \Delta t_{crit} = \frac{T_n}{\pi} \cong \frac{L_{min}}{c} \quad (5)$$

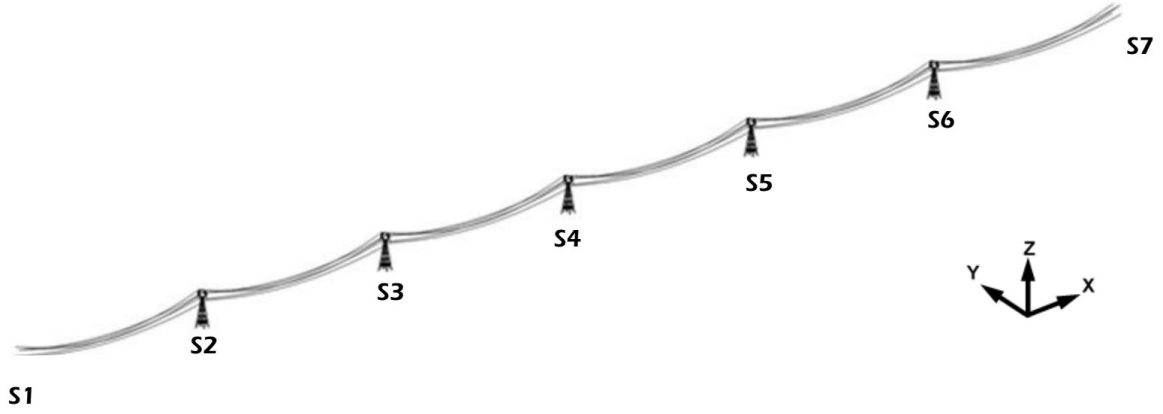


Figure 3: Perspective of the transmission line section.

where  $L_{min}$  is the shortest truss member length in the structure and  $c = \sqrt{E/\rho}$  is the speed of sound in the medium, calculated as the squared root of elastic modulus ( $E$ ) divided by the density of the material ( $\rho$ ).

### Case study

The transmission line section investigated in this case study is a single circuit section, composed of three conductor phases and two shield wires attached to seven supports (S1 to S7), equally spaced by 550m spans, as depicted in figure 3. In order to reduce the computational effort, the dead-end towers were replaced by rigid supports. Return periods adopted for the original TL design were  $T = 50$  years for the design of the components in serviceability limit state (SLS) and  $T = 250$  years in ultimate limit state (ULS).

Suspension supports are freestanding steel latticed towers (named CGA47) with total height of 54.5m a  $14 \times 14$  m squared base. All members are structural steel angle sections, grades 345 MPa or 413 MPa. The self-weight of the tower is approximately 108 kN.

Each conductor phase is composed of a bundle of four Aluminium Cable Steel Reinforced (ACSR) type conductors, commercial name Rail. All phases were sagged according to a catenary parameter of  $C = 1900$  m with an average environmental temperature ( $20^\circ\text{C}$ ) and no wind. Such a weather case is typically referred to as everyday stress (EDS) in standard TL design practice. The horizontal axial tension component in each cable is  $H = 29.82$  kN. In the analysis, the bundle was replaced by an equivalent cable with cross-sectional area, dead weight and ultimate tension capacity (UTC) four times the respective parameters for the single cable.

The shield wires are single cables, also ACSR type, with commercial name Dotterel. A catenary parameter of  $C = 2073$  m was adopted for sagging, also in EDS weather condition, equivalent to  $H = 13.61$  kN. The mesh of cable elements for both conductors and shield wires was automatically generated by dividing the total length of each span into a number of elements with length closest to 25 m.

The suspension insulators of the transmission line section are I-string type on the external phases and V-string type in the internal phase.

A mass-proportional constant of  $c_m = 2\text{ s}^{-1}$  was adopted for the towers and  $c_m = 0.5\text{ s}^{-1}$  for cables, equivalent to a critical damping ratio of  $\zeta = 0.08$  (towers) and  $\zeta = 0.16$  (cables), approximately.

The critical time-step interval was calculated for the shortest element of the towers CGA47 (0.5 m) by means of equation (5),

resulting in  $\Delta t_{crit} \cong 1.0 \times 10^{-4}$  s, adopted for the analyses.

The response of transmission line section was determined for the following loading cases:

- LC1 A simplified wind load is applied transversally to the line section, using a generic wind profile defined by IEC60826. The return period of the wind is  $T = 250$  years (ULS). No conductor breakage is simulated.
- LC2 The conductor breakage is simulated under EDS condition. No wind load is applied.
- LC3 A wind load is applied to the line section, as described for LC1. The return period of the wind is  $T = 50$  years (SLS). The conductor breakage is simulated.
- LC4 As for LC3, but with ULS winds ( $T = 250$  years).

In LC2, LC3 and LC4 the conductor breakage is simulated severing the conductor bundle in right phase of the 1<sup>st</sup> span, by equalling to zero the rigidity of the cable element attached on the insulator of support S2.

The case study site is assumed to be in north-east Brazil, and the meteorological and topographical parameters were adopted accordingly. The roughness of the terrain is category B. The design values of wind speeds ( $V_d$ ) and wind pressures ( $q_d$ ), calculated according to IEC60826, are listed in table 1. In the case of conductors and shield wires, the design values indicated are assumed as constant along the spans. For the supports, they are referred to a height of 10 m, but adjusted according to the height of the panel of interest.

Component	$T = 50$ years		$T = 250$ years	
	$V_d$ (m/s)	$q_d$ (Pa)	$V_d$ (m/s)	$q_d$ (Pa)
Shield Wire	30.62	577.3	36.37	810.7
Conductor	29.61	546.9	35.40	768.0
Supports	29.34	538.0	35.28	762.9

Table 1: Design wind speed and pressure on TL components.

In all load cases, the dead weight is applied gradually for all components of the system, increasing from weightless to the actual weight, over the interval  $t = 0$  s to  $t = 5$  s, remaining constant after that. The wind loads in LC1, LC3 and LC4 are also applied in a similar fashion, from  $t = 5$  s to  $t = 10$  s. At time  $t = 20$  s the conductor bundle is severed, and the interval from  $t = 20$  s to  $t = 50$  s is used in all cases to analyse the dynamic response of the line section.

## Results

For all load cases, the dynamic response of the TL section was determined at each integration time step and recorded at  $5 \times 10^{-2}$ s apart.

The safety of the supports was estimated by calculating the usage factor (UF) of each member, i.e., the relation between the peak dynamic load (PDL) and the respective mechanical capacity (CAP) of the member. A usage factor greater than one indicates that the member was overloaded during the loading event and is unsafe. Note that the unsafe members are kept in the analysis as intact.

The mechanical capacity of the angle section members of towers were calculated according to the methodology of the standard ASCE10-97 - ASCE (2000). It was assumed that the members could only fail due (i) buckling of the gross cross-sectional area or (ii) excessive tension in the net cross-sectional, therefore dismissing any kind of connection failure.

The percentage of unsafe members ( $UF > 1$ ) in supports S2 to S6 obtained in each simulation is listed in table 2, according to the load cases.

SUPPORT	LC1	LC2	LC3	LC4
S2	0	11	26	34
S3	0	0	2	9
S4	0	0	0	3
S5	0	0	0	4
S6	0	0	0	6

Table 2: Percentage of unsafe members of supports S2 to S6.

Similarly, table 3 indicates the maximum usage factor of the members of supports S2 to S6.

SUPPORT	LC1	LC2	LC3	LC4
S2	0.98	2.18	3.17	3.57
S3	0.99	0.80	1.60	1.65
S4	0.98	0.49	0.88	1.16
S5	0.99	0.58	0.91	1.16
S6	0.98	0.59	0.99	1.24

Table 3: Maximum usage factors of supports S2 to S6.

The LC1 is the response of the system to the design conditions (ULS), and no member failure is evident in the supports, as expected. In LC2, 11% of the members in the support closest to the failure point (S2) are unsafe (figure 4), but the remaining supports are undamaged. In LC3, where a SLS wind is applied, the support S2 (26%) is compromised, while S3 (2%) is slightly affected. In the last case, support S2 (34%) is critically compromised, and the all other supports display some unsafe members.

## Conclusions

This paper describes a mechanical model developed to numerically analyse coupled TL sections, employing time-history dynamic analysis to deal with member nonlinearities and changes in boundary condition. The components of the line section are fully simulated, and precise cable elements were adopted for conductors and shield wires. Further enhancements, such as more accurate material constitutive relationships and realistic wind models, can be easily incorporated.

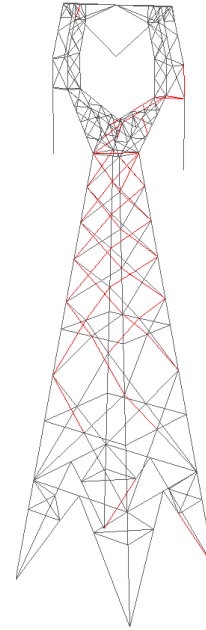


Figure 4: Unsafe members (red) of support S2 for LC2.

The dynamic response of a TL section under four different loading conditions combining conductor failure and wind was obtained. The results clearly indicate that conductor breakage greatly amplifies the response of the system, and the line section become unsafe even under everyday stress condition. In a wind scenario, the TL section is further overloaded, the number of supports affected is expanded and the maximum usage factor is considerably increased.

Therefore, dynamic analysis including conductor breakage is essential in cases where the protection of a line section is imperative, such as large river crossings, for example.

## Acknowledgements

The authors would like to acknowledge the financial support of CNPq - Brazilian National Council for Scientific and Technological Development. \*

## References

- ASCE (2000) ASCE10-97 Design of Latticed Steel Transmission Structures. American Society of Civil Engineers, Reston, VA, DOI 10.1061/9780784403242
- Chopra AK (1995) Dynamics of structures. Prentice Hall New Jersey
- CIGRÉ (1996) Review of IEC 826: Loading and Strength of Overhead Lines. Tech. Rep. December, Conseil International des Grands Réseaux Electriques
- CIGRÉ (2012) Mechanical Security of Overhead Lines - Containing Cascading Failures and Mitigating Their Effects. Tech. Rep. October, Conseil International des Grands Réseaux Electriques
- Groehs AG (2001) Mecânica vibratória. São Leopoldo: Editora Unisinos
- IEC (2003) IEC 60826 - Design Criteria of Overhead Transmission Lines. International Electro Technical Commission